*URSI GASS 2023, Sapporo, Japan, 19 – 26 August 2023*

# UAV-based 3D localization of passive UHF-RFID tags empowering outdoor stock management

Andrea Motroni[(1)], Paolo Nepa [(1)(2)]
(1) University of Pisa, Pisa, Italy; e-mail: andrea.motroni@unipi.it, paolo.nepa@unipi.it
(2) Italian National Research Council (CNR), Turin, Italy

## Abstract

The management of stocks in outdoor warehouses and shipyards is not a trivial task, and UHF-RFID technology represents an attractive candidate to face it. This paper presents the application of a fast 3D Synthetic Aperture Radar (SAR) method sped up through Particle Swarm Optimization (PSO) for localizing goods tagged with passive UHF-RFID tags by exploiting a remotely piloted Unmanned Aerial Vehicle (UAV). The UAV carries reader and antenna and can freely move in the three directions of the space, by forming synthetic arrays with a large aperture length along the three spatial directions. The UAV trajectory is measured through a differential GPS system. Performance is validated through an experimental analysis which demonstrates the feasibility of the proposed system.

## 1 Introduction

The management of outdoor warehouses represents a challenging problem due to the usually large size of the area to be monitored and the large amount of goods [1]. Radio-frequency (RF) technologies can help the warehouse managers by providing location data of the stocks [2].

In outdoor environments, the availability of Global Navigation Satellite Systems (GNSS) allows to implement very effective solutions to monitoring objects such as containers. However, GNSS receivers have a considerable cost and therefore it is necessary to recover the device before shipment to avoid huge expenses. The same happens in case the stocks are equipped with any other battery-powered device, which increases the cost and require a time-consuming battery replacement of discharged devices.

One possible light-weight innovative solution involves the use of passive RFID technology at the Ultra-High Frequency (UHF) band. Due to the very low cost, the almost unlimited lifetime of the tags and the ability to be adapted to any type of surface and material, tagging of numerous objects is possible. The main disadvantage concerns the reading range of these systems, constrained by limits on radiated emissions, which does not allow a reading range above 10-12 m. Warehouses in which a forklift equipped with RFID hardware on board detects the tags of the forked objects are common, even in indoor environments. By tracking the position of the vehicle it is possible to track the position of the objects as well [3]. Alternatively, an Unmanned Aerial Vehicle (UAV) can be equipped with RFID reader and antenna [4–6] to detect and also locate tags. A family of localization techniques that can best exploit the scenario, i.e., leverage the presence of a moving RFID reader, is that of Synthetic Aperture Radar (SAR) localization systems [7]. The principle on which it is based exploits the relative motion between the reader antenna and the tag.

During the motion, the reader collects successive replies from the tags and gathers the phase of the measured signal. Measurements acquired at different locations are combined, so that the antenna is treated as a synthetic array. Such solution allow for decimeter accuracy of goods localization and might be really effective in outdoor warehouses or shipyards. One of these techniques, SARFID [8], has already been validated for 2D [6] and 3D [9] object localization with a drone in flight. The 3D object localization is necessary when the height above ground also needs to be estimated. To overcome the problem of high computational complexity of SARFID in its 3D version, in this paper we propose to enhance the localization method speed through a Particle Swarm Optimization (PSO) algorithm [10, 11], by obtaining the PSO-SAR algorithm. Since in order to apply SARFID or PSO-SAR it is necessary to know the position of the antenna very accurately [12], we measure it by means of a Differential Global Positioning System (DGPS), which allows to achieve much higher accuracy than conventional GPS.

## 2 3D Tag Localization Algorithm

SARFID is a SAR localization method for passive RFID tags at UHF band. In our case, we consider a UAV equipped with a reader and an antenna which flies upon an outdoor warehouse or shipyard. During its flight, a RFID tag located at $\mathbf{p_{tag}} = [x_{tag}, y_{tag}, z_{tag}]^T$ is detected $N_r$ times by the reader with a sampling time $T$ in a subset of its total flight path. The antenna phase center location is without loss of generality here assumed equal to the drone location at each timestep $k$, and it is $\mathbf{A_k} = [a_{x_k}, a_{y_k}, a_{z_k}]^T$, with $k = [0 \dots N_r - 1]$. The antenna forms a synthetic array, which sizes along the three space directions are, are $D_x = \max(a_{x_k}) - \min(a_{x_k})$, $D_y = \max(a_{y_k}) - \min(a_{y_k})$, and $D_z = \max(a_{z_k}) - \min(a_{z_k})$. At the $k$-th timestep, the reader

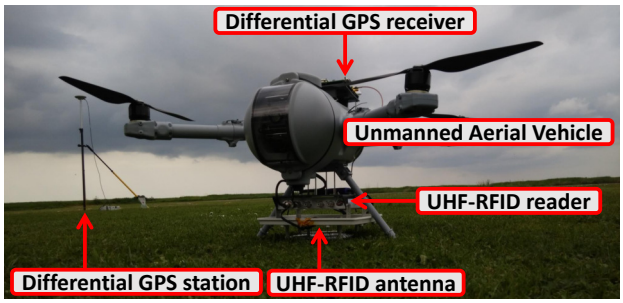


**Figure 1.** Utilized UAV equipped with the GNSS module and UHF-RFID antenna and reader.

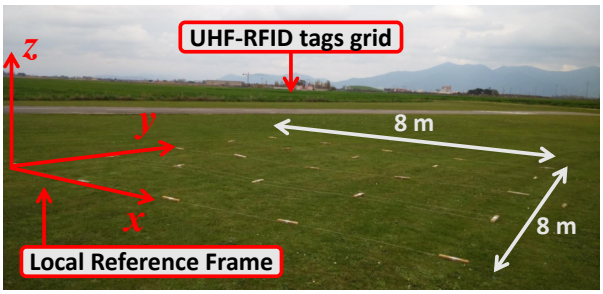


**Figure 2.** Grid of 5 × 5 UHF-RFID tags used in the experiments.

measures a phase sample $\tilde{\theta}_k$ affected by noise:

$$\tilde{\theta}_k = \mathrm{mod}\left(\frac{-4\pi\|\mathbf{A_k}-\mathbf{p_{tag}}\|}{\lambda}+\theta_{off}+n_k, 2\pi\right) \quad (1)$$

where $\lambda$ is the carrier wavelength, $\theta_{off}$ is a phase offset given by the cables and the antenna and tag circuitry, the operator $\|\cdot\|$ calculates the euclidean distance, and $n_k$ is a Gaussian random variable with zero mean defined as $n_k \sim \mathcal{N}(0,\sigma_n^2)$, where $\sigma_n^2$ is the noise variance. The phase is a periodic quantity which completes a round of $2\pi$ each change in distance equal to $\lambda/2$, The offset term $\theta_{off}$ can be canceled by subtracting the first available phase value ($k=0$) from all the others through $\Delta\tilde{\theta}_k = \tilde{\theta}_k - \tilde{\theta}_0$:

Now, a matching function $\mathbf{C}(\mathbf{p}_{\mathbf{tag}}^{i})$ is computed through the following phasor matching:

$$\mathbf{C}(\mathbf{p}_{\mathbf{tag}}^{i}) = \left|\frac{1}{N_r}\sum_{k=0}^{N_r-1} e^{j\Delta\tilde{\theta}_k} e^{-j\Delta\theta_k(\mathbf{p}_{\mathbf{tag}}^{i})}\right| \quad (2)$$

where $\Delta\theta_k(\mathbf{p}_{\mathbf{tag}}^{i})$ is the theoretical value of $\Delta\tilde{\theta}_k$ computed at a hypothetical tag location in the 3D space $\mathbf{p}_{\mathbf{tag}}^{i}$ and with the hypothesis of null noise. $\mathbf{C}(\mathbf{p}_{\mathbf{tag}}^{i})$ function takes real values ranging from 0 to 1.

Then, the tag location is estimated through the following:

$$\hat{\mathbf{p}}_{\mathbf{tag}} = \underset{\mathbf{p}_{\mathbf{tag}}^{i}}{\arg\max}\, \mathbf{C}(\mathbf{p}_{\mathbf{tag}}^{i}) \quad (3)$$

From the Nyquist-Shannon sampling theorem, it is also required for consecutive antenna locations to be less than $\lambda/4$ apart to avoid the occurrence of ambiguous lobes in the matching function.

The search for the hypothetical tag location $\mathbf{p}_{\mathbf{tag}}^{i}$ position that maximizes the matching function can be done by either exhaustive search, as in conventional SARFID, or by faster optimization algorithms such as PSO which can determine the maximum of non-convex functions [11], by obtaining the so called PSO-SAR algorithm. The PSO-SAR is an iterative method and it is here launched to search for the maximum (3) of the matching function (2). To initialize the algorithm, we take in consideration a set of $N_P$ random particles, corresponding to $N_P$ hypothesized values $\mathbf{p}_{\mathbf{tag}}^{i}$ of the tag position $\mathbf{p}_{\mathbf{tag}}$. More details about the PSO algorithm can be found in [10].

## 3 Experimental Analysis

### 3.1 Measurement Setup

The experiment was conducted using the an IDS Colibrì IA-3 microclass UAV drone, (Figure 1) equipped with commercial UHF-RFID hardware. The drone was furnished with a Compact Dual Frequency Board TOPCON B110 GNSS receiver, designed for DGPS use to track the UAV trajectory with a 2 cm accuracy and a time interval of 200 ms.

A CAEN WANTENNAX005 circularly polarized UHF-RFID antenna, and an Impinj Speedway Revolution R420 UHF-RFID reader were installed on the UAV. The reader was powered by the drone battery and transmitted with a power of $P_{TX} = 26$ dB$_\mathrm{m}$ at $f_0 = 865.7$ MHz.

A grid of 25 UHF-RFID dipole-like tags was set up to cover an outdoor space of 8 m × 8 m, as depicted in Figure 2. The tags were deployed according to a 2 m spaced regular pattern. Different tag types were used, including Monza 4 and Monza 6 chips, and two orientations (along $x$-axis and $y$-axis) were tested. The locations of the tags were measured using a GS15 GPS/GLONASS manual total station for comparison with RFID localization output. Both the tags and the UAV locations measured by GPS were converted to a local reference frame.

An example of measured UAV trajectory is reported in Figure 3, which shows a an "almost square-wave path" in the local reference system. The antenna path size is around 8 m along both the $x$-and $y$-directions, and the drone speed varies between 0.1 and 1.3 m/s.

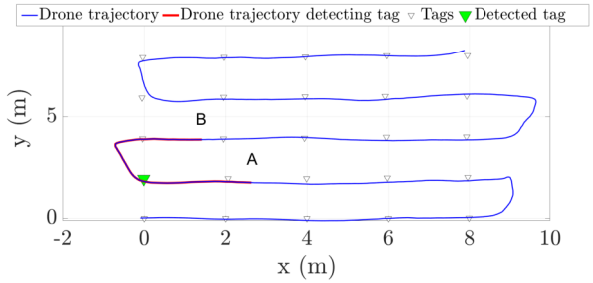


**Figure 3.** Example of the UAV "almost square-wave path" trajectory measured with the GNSS receiver. The highlighted red trajectory portion represents the trajectory data during the detection of a AD-229 tag placed at $\mathbf{p_{tag}} = [x_{tag}, y_{tag}, z_{tag}]^T = [-0.01, 1.95, 0]^T$ m

## 3.2 Results

Let us at first consider the case in which the UAV flies along the "almost square-wave path" of Figure 3 and detects for a portion of its motion an Avery Dennison AD-229 RFID tag located at $\mathbf{p_{tag}} = [x_{tag}, y_{tag}, z_{tag}]^T = [-0.01, 1.95, 0]^T$ m. The tag is detected through a "U" shaped path starting from the point $A = [2.61, 1.76, 2]^T$ m to the point $B = [1.42, 3.88, 2.07]^T$ m composed by $N_r$=364 tag readings. The dimensions of the synthetic array along the $x$-, $y$- and $z$-axis are $D_x = 1.19$ m, $D_y = 2.12$ m, and $D_z = 0.07$ m, respectively. The 3D-SARFID method with exhaustive search is ran by considering a search space of 12 m $\times$ 12 m $\times$ 2 m with a grid step of 2 cm. A total of 601 $\times$ 601 $\times$ 101 = 36.481.301 points is therefore investigated. The estimated 3D tag location by applying the 3D-SARFID method is $\hat{\mathbf{p}}_{\mathbf{tag}} = [\hat{x}_{tag}, \hat{y}_{tag}, \hat{z}_{tag}]^T = [0, 1.94, 0]^T$ m, which coincides with the output of the PSO-SAR method ran with $N_P = 1000$ particles. The 3D matching function is depicted in Figure 4 for the $xy$-plane when $z = z_{tag}$. It can be seen that due to a good size of the synthetic array along the $x$- and $y$-directions, the main-lobe (in yellow) is very narrow and well locates the $x$- and $y$- coordinates of the tag. In fact, the main-lobe shrinks when the synthetic array sizes increase. It can be noticed that the matching function is not convex, and that is why non-convex optimization is required.

A dataset composed by 132 different trajectories detecting the 25 different tags and with different values of sizes of the synthetic array was then analysed to better understand the 3D method performance. The dataset includes several drone flights. Both 3D-SARFID with exhaustive search and PSO-SAR methods are launched. The PSO-SAR method is ran with $N_P = 100$, $N_P = 500$, $N_P = 1000$, $N_P = 5000$ particles. The Cumulative Distribution Function (CDF) of the 3D localization error $\varepsilon_{3D} = \sqrt{\varepsilon_x^2 + \varepsilon_y^2 + \varepsilon_z^2}$, where $\varepsilon_x = \hat{x}_{tag} - x_{tag}$, $\varepsilon_y = \hat{y}_{tag} - y_{tag}$, and $\varepsilon_x = \hat{z}_{tag} - z_{tag}$ is reported in Figure 5 for the traditional 3D-SARFID with exhaustive search (continuous blue line), the PSO-SAR method with $N_P = 100$ (continuous red line), the PSO-SAR method with

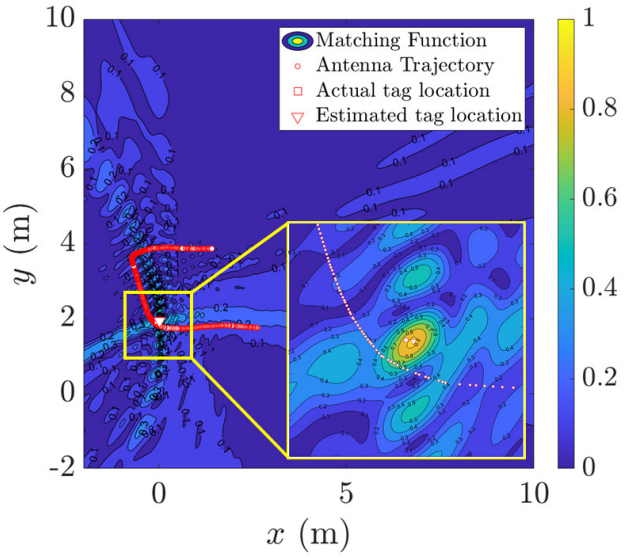


**Figure 4.** 3D matching function vs. the hypothetical tag coordinates for a reader antenna moving along the trajectory depicted in Figure 3 and an RFID tag placed in $\mathbf{p_{tag}} = [x_{tag}, y_{tag}, z_{tag}]^T = [-0.01, 1.95, 0]^T$ m, for the $xy$-plane.

$N_P = 500$ (dashed green line), the PSO-SAR method with $N_P = 1000$ (dotted black line), and the PSO-SAR method with $N_P = 5000$ (dash-dotted magenta line). Unity of measures are expressed in centimeters. The PSO-SAR algorithm is not as performing as the exhaustive search, also because of the large search space in which the particles move. However, the PSO-SAR algorithm has always reached convergence in less than 10 iterations, meaning that in the worst case with $N_P = 5000$, no more than 5000 $\times$ 10 = 50000 hypothetical tag locations were investigated, which is an improvement of a factor 729 with respect to exhaustive search. The performance in terms of mean $\mu_{3D}$ and standard deviation $\sigma_{3D}$ of the location error together with the average processing time $\mu_{PT}$ are shown in Table 1. The advantage of the PSO-SAR method, regardless of the number of particles used, is that it has a much shorter delay due to data processing than the exhaustive search. For this reason, in outdoor warehouses or shipyards, where on average the objects to be located are large and very high accuracy is not required, it might be preferable.

**Table 1.** Mean $\mu_{3D}$ and standard deviation $\sigma_{3D}$ of the localization error, and average processing time $\mu_{PT}$: exhaustive search vs PSO-SAR with different $N_P$ values.

| **Method** | $\mu_{3D}$ (cm) | $\sigma_{3D}$ (cm) | $\mu_{PT}$ (s) |
|---|---|---|---|
| Exhaustive search | 24 | 6 | 64 |
| PSO-SAR with $N_P = 100$ | 44 | 20 | 0.01 |
| PSO-SAR with $N_P = 500$ | 39 | 18 | 0.04 |
| PSO-SAR with $N_P = 1000$ | 39 | 16 | 0.1 |
| PSO-SAR with $N_P = 5000$ | 35 | 15 | 0.4 |

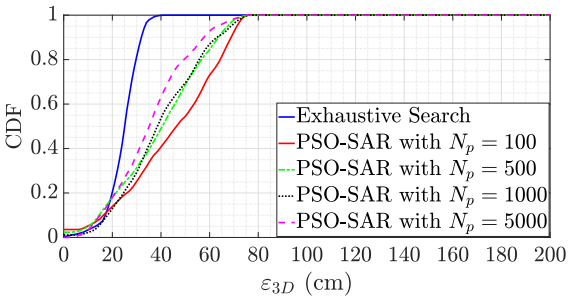


**Figure 5.** Cumulative Distribution Function of the 3D localization error with exhaustive search and PSO-SAR for 132 analysed trajectories.

## 4 Conclusion

This paper presented the application of 3D-SARFID, a localization method for passive UHF-band RFID tags based on the principle of synthetic aperture radar, with the goal of tracking the 3D location of goods in outdoor environments. To demonstrate the feasibility of the solution, antenna and reader were installed on a commercial drone (UAV) that flew over the area detecting the tags multiple times. The position of the antenna was measured using a DGPS system. 3D-SARFID can be sped up through a PSO method, which allow shorten the processing time and get real-time awareness of the objects location. The obtained performance shows the method effectiveness, which is suitable for localization of items in outdoor warehouses or shipyards.

## References

[1] G. Misahuaman, A. Daza, and E. Zavaleta, "Web-based systems for inventory control in organizations: A Systematic Review," in *2021 IEEE/ACIS 22nd International Conference on Software Engineering, Artificial Intelligence, Networking and Parallel/Distributed Computing (SNPD)*, Nov. 2021, pp. 15–20, doi: 10.1109/SNPD51163.2021.9704993.

[2] M. Gareis, A. Parr, J. Trabert, T. Mehner, M. Vossiek, and C. Carlowitz, "Stocktaking Robots, Automatic Inventory, and 3D Product Maps: The Smart Warehouse Enabled by UHF-RFID Synthetic Aperture Localization Techniques," *IEEE Microwave Magazine*, vol. 22, no. 3, pp. 57–68, 2021, doi: 10.1109/MMM.2020.3042443.

[3] A. Motroni, A. Buffi, and P. Nepa, "Forklift Tracking: Industry 4.0 Implementation in Large-Scale Warehouses through UWB Sensor Fusion," *Applied Sciences*, vol. 11, no. 22, 2021, doi: 10.3390/app112210607.

[4] C. Li, E. Tanghe, P. Suanet, D. Plets, J. Hoebeke, E. De Poorter, and W. Joseph, "ReLoc 2.0: UHF-RFID Relative Localization for Drone-Based Inventory Management," *IEEE Transactions on Instrumentation and Measurement*, vol. 70, pp. 1–13, 2021, doi: 10.1109/TIM.2021.3069377.

[5] G. Casati, M. Longhi, D. Latini, F. Carbone, S. Amendola, F. Del Frate, G. Schiavon, and G. Marrocco, "The Interrogation Footprint of RFID-UAV: Electromagnetic Modeling and Experimentations," *IEEE Journal of Radio Frequency Identification*, vol. 1, no. 2, pp. 155–162, 2017, doi: 10.1109/JRFID.2017.2765619.

[6] A. Buffi, A. Motroni, P. Nepa, B. Tellini, and R. Cioni, "A SAR-Based Measurement Method for Passive-Tag Positioning With a Flying UHF-RFID Reader," *IEEE Transactions on Instrumentation and Measurement*, vol. 68, no. 3, pp. 845–853, 2019, doi: 10.1109/TIM.2018.2857045.

[7] H. Liu, Y. Ma, Y. Jiang, Y. Zhang, and X. Liang, "On Fast and Accurate 3D RFID Mobile Localization," in *2021 IEEE International Conference on RFID (RFID)*, 2021, pp. 1–8, doi: 10.1109/RFID52461.2021.9444375.

[8] F. Bernardini, A. Buffi, D. Fontanelli, D. Macii, V. Magnago, M. Marracci, A. Motroni, P. Nepa, and B. Tellini, "Robot-Based Indoor Positioning of UHF-RFID Tags: The SAR Method With Multiple Trajectories," *IEEE Transactions on Instrumentation and Measurement*, vol. 70, pp. 1–15, 2021, doi: 10.1109/TIM.2020.3033728.

[9] A. Buffi and B. Tellini, "Measuring UHF-RFID Tag Position via Unmanned Aerial Vehicle in Outdoor Scenario," in *2018 IEEE 4th International Forum on Research and Technology for Society and Industry (RTSI)*, 2018, pp. 1–6, doi: 10.1109/RTSI.2018.8548428.

[10] J. Kennedy and R. Eberhart, "Particle swarm optimization," in *Proceedings of ICNN'95 - International Conference on Neural Networks*, vol. 4, 1995, pp. 1942–1948 vol.4, doi: 10.1109/ICNN.1995.488968.

[11] F. Bernardini, A. Buffi, A. Motroni, P. Nepa, B. Tellini, P. Tripicchio, and M. Unetti, "Particle Swarm Optimization in SAR-Based Method Enabling Real-Time 3D Positioning of UHF-RFID Tags," *IEEE Journal of Radio Frequency Identification*, vol. 4, no. 4, pp. 300–313, 2020, doi: 10.1109/JRFID.2020.3005351.

[12] G. Bandini, A. Motroni, A. Buffi, M. Marracci, and B. Tellini, "On the Effect of Position Uncertainty of the UHF-RFID Reader Trajectory in SAR-based Localization via UAV," in *2022 IEEE International Symposium on Measurements Networking (MN)*, 2022, pp. 1–6, doi: 10.1109/MN55117.2022.9887773.